

# Novel Integrity Concept for CAT III Precision Approaches and Taxiing: Extended GBAS (E-GBAS)

Wolfgang Schuster and Washington Ochieng

(*Centre for Transport Studies, Imperial College London*)

(Email: w.schuster@imperial.ac.uk)

Future air navigation envisages increased use of Global Navigation Satellite Systems (GNSS) together with advanced communications and surveillance technologies to facilitate the required increase in capacity, efficiency and safety without adversely impacting the environment. The full benefit of GNSS is expected from its ability to support en-route to en-route or gate-to-gate air navigation. This presents challenges particularly for the phases of flight with stringent required navigation performance. Significant work has so far been devoted to the phases of flight up to CAT I. However, more work is required for CAT III precision landing (with an accuracy requirement at the metre level) and taxiing (with an accuracy requirement at sub-metre level) and both with very high integrity and continuity requirements. The main limitation in using GBAS for CAT III landings is the potential decorrelation of the measurement errors between the GBAS ground station (GGS) and the user. The threats in this respect are the atmospheric anomalies. Periods of strong solar activity can cause large local spatial and temporal gradients in the delays induced on the GNSS signals by the ionosphere. The local nature of the effects results in significant decorrelation between GGS measurements and the user. Therefore, a reliable ground based ionospheric anomaly monitoring scheme is required to guarantee integrity.

This paper critically reviews state-of-the-art monitors, identifies their limitations and addresses them by proposing a high-performance monitoring scheme for the ionosphere. Preliminary analyses suggest that the proposed scheme has the potential to enable GNSS to meet the navigation requirements for CAT III and taxiing.

## KEY WORDS

1. CAT III.
2. E-GBAS.

1. INTRODUCTION. The ionosphere extends in various layers in a region spanning a height between 50 km and 1000 km above the Earth's surface. It is a dispersive medium in which free electrons and ions produced by solar radiation cause a phase advance and a group delay of GNSS signals. The magnitude of the delays is determined mainly by the density of the free electrons (sometimes referred to as Total Electron Content or TEC) (Hoffman-Wellenhof et al, 2001). Although usually highly correlated over short distances, during periods of high solar activity, rapid changes in the TEC can occur both spatially and temporally, leading to significant



Figure 1. Smoothing filter (adapted from Konno et al., 2006a).

decorrelation over short distances, with observed magnitudes of at least 400 mm/km. However, the agreed threat-space for CAT III landings is still under review (Konno et al, 2006a).

Moreover, the result of rapid local fluctuations in the TEC results in a phenomenon called “Ionosphere scintillations”. These scintillations are associated with periods of high solar activity, but can also be associated with strong aurora in the high latitude regions, persisting even during periods of solar minimum. These TEC fluctuations are typically observed as rapid and random variations in the phase and amplitude of the GNSS signals (Skone et al, 2005). This can result in either loss-of-lock (e.g. as a result of significant variations in the signal-to-noise ratio), or cycle slips (as a result of phase changes). Loss-of-lock requires a reacquisition of the signal and may lead to a loss of continuity and cycle slips which are of particular concern for carrier-phase based high accuracy and high integrity navigation algorithms.

The emphasis in this paper is on the detection and mitigation of ionosphere fronts as they have the potential to adversely affect GNSS-based air navigation operations in the mid-latitude regions of Europe and the USA. The paper starts by reviewing the state-of-the-art monitors currently proposed to mitigate the risks associated with ionosphere fronts. The limitations of the monitors are then identified and new monitoring algorithms proposed to address them.

**2. STATE-OF-THE-ART IONOSPHERE MONITORING.** Current algorithms for CAT I approaches are based on the use of single-frequency code measurements at user level corrected with measurements from the GBAS Ground Station (GGS). This method assumes that the measurements between the user and the GGS are highly correlated. However, spatial decorrelation of the ionosphere-induced delays can reach levels of the order of at least 400 mm per kilometre distance between the GGS and the user (Konno et al, 2006a). As a result, there is the potential for large uncertainties in the corrected user measurements. Moreover, the code measurements are inherently noisy creating residual uncertainties at the metre-level (Schlueter et al, 2005; Konno 2006b). In order to “smooth” the noise, a filter is typically applied, making use of single-frequency carrier-phase measurements. The general form of such a filter is shown in Figure 1.

Furthermore, the use of single-frequency observables suffers from additional uncertainties in the ionosphere delay due to temporal gradients in the ionosphere. These are potentially large since as stated earlier, ionosphere fronts may have gradients at the level of 400 mm/km or higher and move at a speed of up to approximately 0.75 km/s (Konno et al, 2006a). This results in potential variations of the ionosphere-induced delay at a given location of  $\sim 300$  mm/s. These are effectively averaged out over the smoothing time of the filter, as shown in the

following equation:

$$\bar{\Psi} = r + (2F - 1)I_{1,j}^i + F\eta_{1,j}^i \quad (1)$$

Both potential spatial and temporal gradients can result in large uncertainties in the final user measurements, significantly above the performance requirements for CAT III landings (EUROCAE, 2007; RTCA, 2004).

Various studies have been carried out to mitigate the risks associated with ionosphere anomalies in order to meet the stringent CAT III requirements. Datta-Barua et al (2006) developed a method to bound the errors that arise as a result of ignoring higher order terms (i.e. as a result of employing first order ionospheric error correction) using dual frequency data. Konno et al. (2006b), representing the state-of-the-art attempt to mitigate these risks using two dual-frequency methods: DFree (Divergence-free) and IFree (Ionosphere-free), as explained in Section 2.1. DFree was found to be superior under most conditions, except extremely anomalous conditions, where IFree was shown to be superior. In order to monitor the ionosphere status and determine which method to use, Konno et al. (2006a) developed a dual-frequency method to monitor the ionosphere behaviour between the GGS and the user. This method combines two algorithms: the first estimates the temporal gradients using dual-frequency carrier-phase and the second computes the spatial gradients between the GGS and the user using dual-frequency code-based measurements, as described in detail in Section 2.2.

2.1. *Overview.* The functional architecture of the method used in Konno et al (2006a, 2006b) to mitigate the risks induced by the ionosphere is shown in Figure 2. The method is essentially divided into two parts:

- mitigation under nominal conditions using the DFree and IFree methods to reduce the overall uncertainty introduced by the ionosphere (under the assumption that the state of the ionosphere is known – i.e. that monitors exist), and
- monitoring of the ionosphere to exclude affected satellites and compute protection levels under non-nominal ionosphere conditions.

The dual-frequency observables used by Konno et al. (2006b) in determining the ranges is based on the use of divergence-free (DFree) and ionosphere-free (IFree) smoothing. The objective of smoothing is to minimise the noise on the code measurements using the less noisy carrier-phase measurements.

DFree removes the temporal gradients from the ionospheric delay using dual frequency carrier phase measurements to smooth the code measurements. However, spatial ionospheric gradients are not removed with the DFree method. Therefore, Konno et al. (2006b) propose an alternative method, IFree smoothing, which removes the spatial and temporal effects using linear combinations of dual-frequency code and carrier measurements. However, the method suffers from noisy outputs from the smoothing filter, resulting in reduced availability. Therefore, the optimal choice of the smoothing method depends on the state of the ionosphere. Under nominal conditions, Konno et al. (2006b) show that DFree smoothing leads to a higher availability. Conversely, under strong ionosphere anomaly conditions the IFree provides a higher availability, only limited by the receiver error models and the alert limits. In order to optimally combine these two smoothing algorithms, a monitor is needed to track the

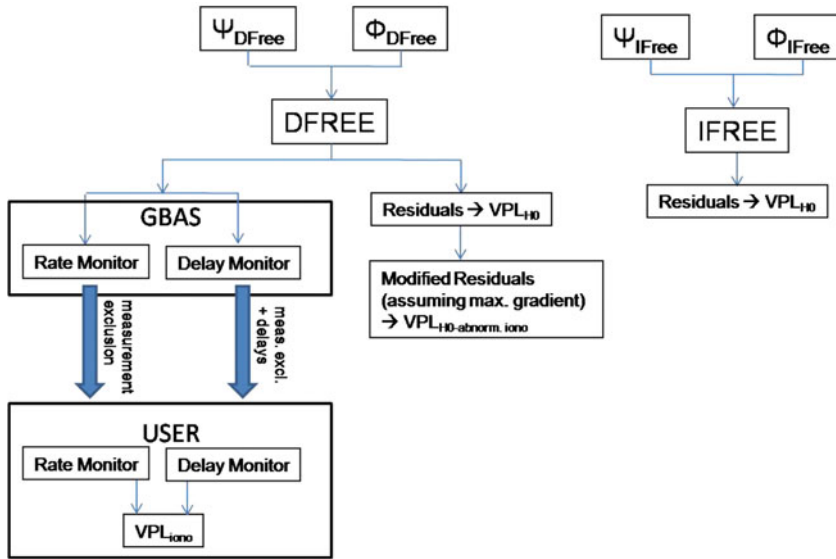


Figure 2. Functional architecture of Ionosphere monitoring in (Konno et al., 2006a, b) measurement observables.

state of the ionosphere and provide an alert to switch between the DFree and IFree smoothing methods.

The relevant results obtained in Konno et al. (2006b) are summarized as follows:

- The DFree algorithm, under nominal ionosphere conditions, reaches an availability of 98.7% if a VAL = 5.3 m is assumed. This is below the minimum availability requirements of 99.9% for CAT-III approaches. A VAL = 2.6 m (as specified by EUROCAE, 2007) would lower this further.
- The IFree algorithm, with improved Airborne Accuracy Designator B (AAD-B) and Ground-Accuracy Designator C (GAD-C) error properties, by 75% and 50% respectively, produces a maximum availability of 98.4% with a VAL = 5.3 m. Again, a VAL = 2.6 m will result in a lower availability.

In order to determine the state of the ionosphere and choose the appropriate smoothing method, Konno et al. (2006a) propose a monitoring architecture (depicted in Figure 2) and described in the next Section.

**2.2. Ionosphere Monitoring.** Konno et al. (2006a) propose two ionosphere monitors based upon measurements of the temporal and spatial gradients of the ionosphere delays at both the GGS and the user locations: rate-based and delay-based monitors. In the former, the temporal gradients are computed using dual-frequency carrier-phase measurements and are then converted to spatial gradients making the assumption that ionosphere fronts can be modelled in terms of a gradient, a width and a velocity. The drawback is that if the Ionosphere Pierce Point (IPP) moves with the same velocity as the ionosphere front, no time variations and hence no spatial variations are detected. To compensate for this undetectable condition, Konno et al. (2006a) introduce the delay-based algorithm that directly computes the ionosphere spatial differences using dual frequency code measurements. These are double

differenced, to remove the Inter-Frequency Bias (IFB), and carrier-phase-smoothed, to reduce the noise. The assumption is made that both the user and the GGS have the same ionosphere monitor.

The rate-based monitor estimates temporal gradients using dual-frequency carrier-phase measurements. As identified in Konno et al. (2006a), a potentially hazardous situation occurs when the front and IPP velocities align, making it impossible for the rate-based ionosphere monitor to detect this threat. Konno et al. (2006a) conclude that a front that moves with the IPP of the user and hits the IPP of the GGS just as the user passes the decision point is the most severe undetectable condition with this monitor. This is applicable to fronts affecting any number of satellites, although in practice such alignment has only been observed for up to two satellites. As a result of this deficiency, the delay-based monitor was developed based on the comparison by the user of the ionosphere-induced delays computed and broadcast by the GGS with those computed by the user. However, the approach has the weaknesses of errors from high noise levels and the difference in inter-frequency bias between the GGS and user receivers (the satellite hardware group delay is common to both GGS and user and hence cancels out). The IFB is cancelled out by double differencing with the highest satellite.

*2.3. Current Limitations.* The method developed in Konno et al. (2006a) combines the rate-based algorithm with the delay-based algorithm to monitor the ionosphere. Theoretically, it allows switching between the DFree user algorithm under nominal ionosphere conditions and the IFree algorithm under ionosphere anomaly conditions. Furthermore, it allows optimisation of service availability by using the satellite exclusion of the monitors as well as the computation of standard and enhanced Vertical Protection Levels (VPLs). However, there are a number of limitations to this approach:

- The IFree method can only support a Vertical Alert Limit (VAL) larger than  $\sim 10$  m if error levels of the GGS and user receivers are improved by up to 75% with respect to current levels, in order to satisfy CAT III minimum service availability requirements (99.9%). In particular, the availability of CAT III approach service with the IFree algorithm with a VAL  $\sim 5.3$  m, and assuming current GGS and user receiver error specifications, is at the level of 0.001%. In order to meet the 99.9% availability requirement specified by the RTCA (2004) and EUROCAE (2007), the VAL assumption, which is already larger than the 2.6 m requirement by EUROCAE (2007), would need to be relaxed significantly further. The availability can be shown to increase to 99.977% if the ground errors are improved by 50%, the airborne errors by 75% and the VAL is relaxed to 10 m. In order to be beneficial, significant reduction in receiver errors and relaxation of VAL are required. Whilst the former is likely to be achieved in the future, a relaxation of the VAL is not in line with developments by EUROCAE (2007).
- The baseline (rate-based monitoring) and enhanced (rate-based and delay-based) systems can only support a VAL of 16.5 m and 14.5 m respectively to reach the CAT III minimum service availability of 99.9% (Konno et al., 2006a). This is significantly larger than the VAL = 2.6 m proposed by EUROCAE (2007) and also larger than the VAL = 10 m proposed by the RTCA.

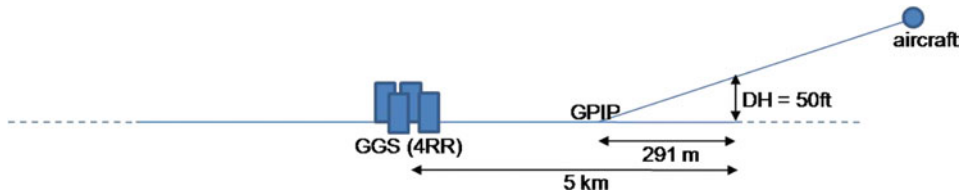


Figure 3. GBAS CAT III – Basic architecture.

- The rate-based monitor algorithm is unable to detect fronts where the satellite IPPs all align with and move at the same velocity as the front. Moreover, the assumption is made that this scenario is limited to two satellites. Although scenarios with more than two satellites have not been observed based on the study results of three cities within the CONTinental United States (CONUS), there is no guarantee that such scenarios do not exist. Additionally, if ionosphere-induced errors for more than two satellites lie under the minimum detection threshold of the rate-based monitor, they are potentially not detected. As a result, it is unclear whether the rate-based monitor is in fact able to limit the affected number of satellites to two.
- The delay-based monitor suffers from large noise errors and inter-frequency biases. The removal of the latter using double differencing leads to the exclusion of at least two satellites simultaneously, raising questions about the impacts on the continuity of service. Moreover, implications for the comparisons with other satellites need to be carefully addressed.
- The reliability of ionosphere monitors could be compromised by unknown ionosphere anomalies since a maximum bias of 400 mm/km together with a nominal dispersion of 5 mm/km is currently assumed in the computation of the VPL.

Given the limitations of the methods described above, Section 3 develops a new method, that has the potential to significantly mitigate the risks associated with ionosphere fronts. Whilst a detailed study of the performance of the proposed method is beyond the scope of this paper, a high level analysis of the expected improvements over the current state-of-the-art is given in Section 3.3.

**3. EXTENDED GBAS (E-GBAS).** Figure 3 presents the basic architecture for CAT III landings as assumed in Konno et al. (2006b). Somewhere on the airport close to the centre, there is an arrangement of four closely spaced reference receivers (RRs) that represent the core GGS and which are used to compute the differential corrections that are transmitted to the aircraft using the Very High Frequency (VHF) Data Broadcast (VDB). The aircraft is on a given descent slope, crossing the threshold at the Decision Height (DH) and intersecting the runway at the Glide Path Intercept Point (GPIP).

The GBAS computes corrections to the direct line-of-sight signal between the satellites and its reference receivers. However, the corrections may be different from

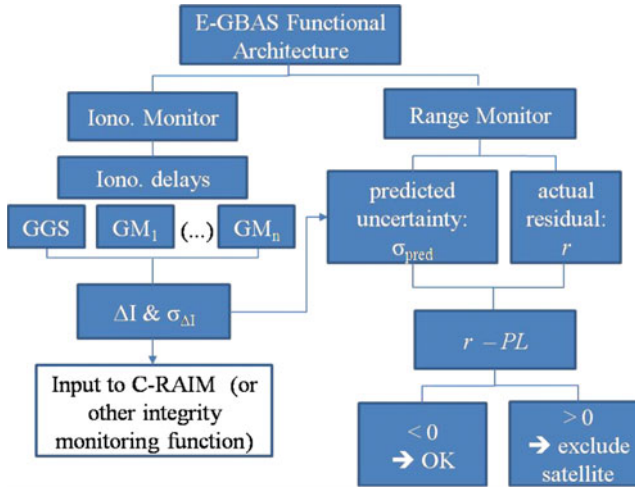


Figure 4. E-GBAS monitor functional architecture.

those of the direct line-of-sight signals between the satellites and the aircraft due to differences in the error magnitudes. The main limitations to this architecture are the potential decorrelations between the errors affecting the GGS and the aircraft. Strong decorrelation of the ionosphere (up to 400 mm/km) has been observed and there is no guarantee that larger decorrelations do not exist. As a result, it is clear that enhanced monitoring techniques are required to mitigate these risks. Monitoring can be done in either the position or range domain. Both of these techniques are discussed as part of the proposed Enhanced GBAS (E-GBAS) architecture developed below.

3.1. *Functional Architecture.* Figure 4 presents the proposed functional architecture for E-GBAS. The introduction of additional monitors into the GBAS architecture serves two purposes: to accurately monitor the ionosphere and to minimise potential decorrelations between aircraft and GGS. Furthermore, it is to provide an overall estimate of the range uncertainty in the corrected data at aircraft level, hence providing additional redundancy, with the potential to increase availability.

3.1.1. *Ionosphere Monitor.* The ionosphere monitor directly estimates the ionosphere delays using dual-frequency carrier-phase measurements:

$$\begin{aligned} \tilde{I}(t) &= \frac{1}{\alpha} (\phi_2(t) - \phi_1(t)) \\ &= I_{1,j}^i(t) + \frac{1}{\alpha} (\tau_{21}^i(t) + IFB_{21,j}(t) + \Delta v_{21,j}^i(t) + \Delta N_{21,j}^i(t)) \end{aligned} \tag{2}$$

where:

$$\alpha = 1 - f_1^2 / f_2^2$$

$\phi$  = carrier-phase observable

$I_{1,j}^i$  = ionosphere advance of L1 carrier

$\tau_{21}^i$  = hardware group delay between L1 & L2 carrier

$IFB_{21,j}$  = interfrequency bias between L1 & L2 carrier



$\Delta v_{21,j}^i =$  difference in carrier-phase noise and multipath between L1 & L2 carrier

$\Delta N_{21,j}^i =$  difference in carrier-phase ambiguity between L1 & L2 carrier

Since the difference in ionosphere delays between the GGS and the GMs is of interest, the satellite hardware group delay  $\tau_{21}$  disappears:

$$\begin{aligned} \Delta_{GM_n-GGS} \tilde{I}(t) &= \tilde{I}_{GM_n}(t) - \tilde{I}_{GGS}(t) \\ &= \Delta_{GM_n-GGS} I_{1,j}^i(t) + \frac{1}{\alpha} \begin{pmatrix} \Delta_{GM_n-GGS} IFB_{21,j}(t) \\ + \nabla_{GM_n GGS} \Delta v_{21,j}^i(t) \\ + \nabla_{GM_n-GGS} \Delta N_{21,j}^i(t) \end{pmatrix} \end{aligned} \quad (3)$$

Given that the GMs and the GGS are stationary, reliable ambiguity resolution and cycle slip detection can be achieved. The uncertainty in the estimate of the difference in ionosphere delays between the GGS and the GMs is given by:

$$\sigma_{\Delta I}^2 = \sigma_{\Delta IFB}^2 + \sigma_{\nabla \Delta v}^2 \quad (4)$$

The uncertainties associated with the Inter-Frequency Bias (IFB) are of the order of a few millimeters for carrier-phase L1 and L2 (Liu et al, 2004) and can therefore be neglected. The same applies for a combination of GPS L1 and L5 as well as the corresponding Galileo signals. The uncertainty in the difference in ionosphere-delay estimations is thus essentially determined by the carrier-phase noise and multipath.

The expected ionosphere bias between the GGS and the aircraft as well as the remaining uncertainties can be extrapolated from the individual ionosphere delay measurements at the GMs and the GGS. The bias is corrected for in the positioning algorithm, and the uncertainty used in the computation of the protection levels. An alternative (more conservative method) would be to use the maximum gradient within the coverage area to compute the maximum bias in ionosphere delay between the GGS and the aircraft in the computation of the protection levels.

The VPL at aircraft level is computed from the above ionospheric uncertainties (Equation 4) as well as the remaining uncertainties (troposphere, code noise at aircraft and GGS), adding the maximum bias that could go undetected with the given monitor configuration. Using the DFree configuration of (Konno et al., 2006b) to compute the differentially corrected ranges at aircraft level, the corresponding vertical protection level is computed as:

$$VPL = K_{ffmd} \cdot \sqrt{\sum_{i=1}^N s_{v,i}^2 \left( \sigma_{\eta,air,DFree}^2 + \sigma_{\eta,GGS,DFree}^2 + \sigma_{Tropo,DFree}^2 + \sigma_{\Delta I}^2 \right)} + \text{Bias}_{\max} \quad (5)$$

where  $K_{ffmd}$  is the fault-free detection multiplier determined from the maximum allowable integrity risk. The maximum bias is determined from the maximum gradient of the allocated threat-space and the maximum distance between the aircraft and the closest baseline joining either two GMs or one GM and the GGS:

$$\text{Bias}_{\max} = \text{gradient}_{\max} \cdot D_{DH-Baseline} \quad (6)$$

In case of a configuration with four GMs as shown in Figure 7 (See Section 3.2.2), this bias would be zero at the decision height for CAT III precision approaches.

3.1.2. *Range Monitor.* The range monitors serve as an additional safeguard, and have the potential to increase service availability for those cases in which an individual



failure mode leads to unavailability as a result of the PL exceeding the alert limit, whilst the overall integrity risk is still met (as a result of the other errors being below their maximum limits). Each GM corrects its own measurements with the differential corrections (corrected for the difference in ionosphere delays between the two stations) provided by the GGS, to extract the corrected range:

$$\begin{aligned} c\bar{\Psi}_{GMn,DFree}^i &= \bar{\Psi}_{GMn,DFree}^i - \left( \bar{\Psi}_{GGS,DFree}^i - R_{GGS,DFree}^i \right) \\ &= R_{GMn}^i + \Delta_{GMn-GGS}t_1 + \Delta_{GMn-GGS}T_1^i + \Delta_{GMn-GGS}I_1^i + F\Delta_{GMn-GGS}\eta_1^i \end{aligned} \quad (7)$$

where

$$\begin{aligned} c\bar{\Psi}_{GMn,DFree}^i &= \text{differentially corrected DFree - smoothed GM n observable} \\ \bar{\Psi}_{GMn,DFree}^i &= \text{DFree - smoothed GM n observable} \\ \bar{\Psi}_{GGS,DFree}^i &= \text{DFree - smoothed GGS observable} \\ R_{GGS,DFree}^i &= \text{True distance between GGS and satellite } i \\ R_{GMn,DFree}^i &= \text{True distance between GM n and satellite } i \\ \Delta_{GMn-GGS}t_1 &= \text{time-offset of GM n with respect to GGS} \\ \Delta_{GMn-GGS}T_1^i &= \text{difference in troposphere delay between GM n and GGS} \\ F &= \text{smoothing factor} \\ \Delta_{GMn-GGS}\eta_1^i &= \text{difference in noise between GM n and GGS} \end{aligned}$$

The corrected ranges are compared to the true ranges to the satellite (from the known GM locations). The measured residual errors are compared to the estimated residual errors, computed based upon the measurement noise, multipath, as well as the ionosphere and troposphere uncertainties. Provided that the measured residual errors are smaller than the estimated residual errors, the satellite is considered healthy. Otherwise, the satellite is excluded.

3.2. *Physical Architecture.* This section discusses considerations and assumptions for building a physical monitoring architecture capable of satisfying the E-GBAS functions described in Section 3.1, for precision approaches and airport surface movement. In the development of the monitor architecture in the following sections, the following assumptions are made on the ionosphere fronts:

- they can be described by a velocity vector, a gradient (in two dimensions) and a width;
- they are wider than the GGS to Ground Monitor (GM) distances.

Furthermore, the proposed architecture accounts for performance requirements, operational constraints and cost. From an operational perspective, the proposed architecture must be able to satisfy all performance requirements of CAT III landings and Airport Surface Movement (ASM). Operational constraints, such as masking satellites visible to the monitors by approaching aircraft, or induction of multipath by aircraft at the monitors, must be given due consideration. Finally, it is clear that any architecture will be a trade-off between the performance it can achieve and the costs incurred.

3.2.1. *Performance Considerations.* The main issue with the current architecture is that decorrelation between the errors at the GGS and at user level pose a significant integrity threat. This should be mitigated by an appropriately designed architecture.

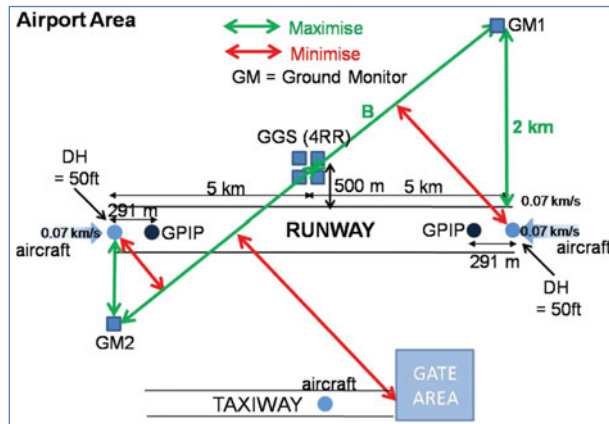


Figure 5. Airport with two GMs.

Ideally, one would locate a monitor at the Decision Height (DH) of the aircraft on approach and compute the ionosphere induced delay at this monitor as well as the GGS. If neither GGS nor the Ground Monitor (GM) detects any ionosphere anomaly, then there would be no ionosphere integrity risk for the user at the DH either. However, for practical reasons, such an architecture is not viable as aircraft on the approach would constantly mask the satellites in view of the GM. Moreover, multipath from the aircraft would also be expected to significantly impact the operation of the monitors. Therefore, the GM should be offset from the DH. Larger offsets minimise the risks of shadowing and multipath. At the same time however, the larger the offset, the larger the potential decorrelation between the GM ionosphere delay measurements and the ionosphere delays affecting the aircraft. Therefore, there are two trade-offs to be made:

- Minimum DH to GM distance for best correlation of errors
- Maximum DH to GM distance for minimum risk of loss of lock (continuity risk) and minimum risk of multipath

Additionally, maximum GM to GGS distances are desirable to optimise the monitoring sensitivity (“lever-arm effect”) of the E-GBAS architecture.

In order to protect against all ionosphere fronts, the architecture should be designed such that it is not possible for a front to affect only the GGS without affecting the GM. This limits the minimum number of GMs needed to two, in order to “cover” the GGS. With such a configuration, the two monitors would have to be placed on opposite sides of the GGS and in one line (see Figure 5). The disadvantage of such a configuration is that the minimum distance between the baseline, connecting GM1 and GM2, and the DH is still relatively large unless the GMs are placed close to the threshold, hence making the GMs prone to masking and multipath by aircraft. Therefore, in order to “cover” (i.e. protect) the GGS and reduce the uncertainties in the decorrelations between the GGS and the user, the minimum configuration should consist of three GMs. The proposed configurations are shown in Figure 6. GM3 could be placed on either side of the runway.

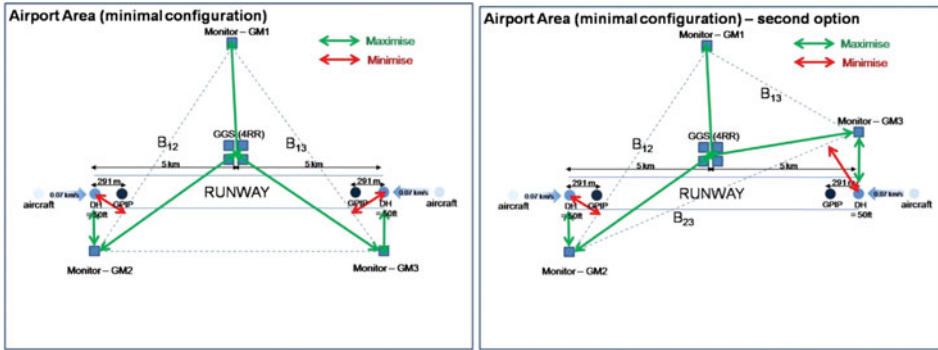


Figure 6. Airport with three GMs – Proposed minimum configuration.

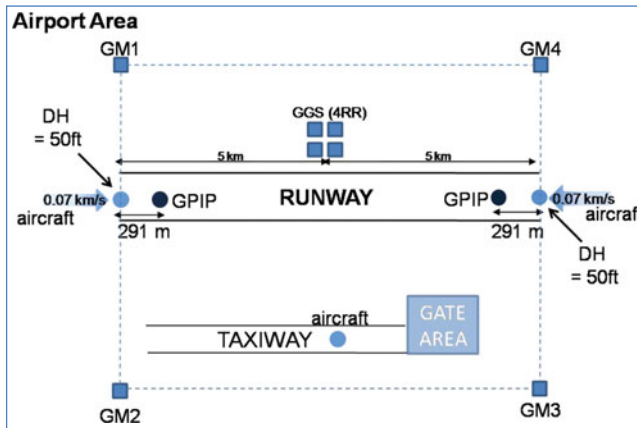


Figure 7. Optimal monitor architecture.

3.2.2. *Operational and Financial Constraints.* In order to minimise multipath and masking by aircraft, the GMs should be placed not only sufficiently far from the approach path, but also from the taxiways and buildings. This may suggest that the minimal configuration of Figure 6 may not be sufficient since a larger distance of the GMs to the DH also results in a larger distance between the closest baseline and the DH. As a result, the optimal configuration of such monitor architecture should consist of four GMs, placed such that most of the airport surface is covered, as shown in Figure 7. From a financial perspective, the architecture should be limited to the minimum possible, whilst meeting the operational and environmental constraints.

3.2.3. *Trade-Offs.* The optimal architecture is a trade-off between the performance, operational and financial considerations. Judging by the stringency of the CAT III approach requirements and the fact that the same architecture would likely also be required to satisfy the much more stringent surface movement requirements, it is unlikely that a two-GM architecture would be sufficient. A detailed analysis would be required to determine whether a three-GM architecture would be sufficient to meet the CAT III and surface movement requirements. A four-GM architecture is optimal

from a performance point of view, given that all the points on the airport with the most critical requirements (such as the DH for CAT III landings, and the gate area for surface movement) are covered. Additionally, if the GMs are placed as shown in Figure 7, the baseline between two monitors passes through the DH and therefore allows a reliable assessment of the ionospheric delay at that point.

3.3. *Expected Performance.* A detailed analysis to quantify the performance of the proposed architecture is beyond the scope of this paper. However, a comparison of the residual errors of the method proposed in this paper and the one in Konno et al. (2006a) is presented here. There are several essential differences between the approach that uses the DFree method with the monitoring schemes described in Konno et al. (2006a), and a configuration where DFree is used together with an E-GBAS architecture. Firstly, the E-GBAS architecture is ground based and uses dual frequency carrier-phase measurements, and thus able to very accurately determine the ionospheric delays and uncertainties. Secondly, the first approach suffers from the following main drawback: in order to optimally switch between the DFree and IFree algorithms reliable ionosphere-anomaly monitors are required. Two such monitors to be used in tandem are proposed in Konno et al (2006a). The first, a rate-based algorithm is very sensitive to ionosphere variations, but is not able to reliably detect ionosphere fronts with small differences in speed between the ionosphere pierce point (IPP) and the front. The second monitor is not very sensitive as a result of the relatively large noise levels associated with using double-differenced dual-frequency code measurements, and the need to make various assumptions with respect to maximum potential biases that may be remaining between the GGS and the user. On the other hand, the use of DFree with a suitable E-GBAS architecture configuration is expected to reliably detect all ionosphere fronts with a high degree of sensitivity, and to eliminate the need to make assumptions with respect to potential biases between the aircraft and GGS. It thereby maximises service availability. Thirdly, the E-GBAS architecture provides enhanced availability if used additionally, as a range monitor.

The first two differences suggest that the contribution of the ionosphere-induced uncertainty in the availability computation is expected to be minimal, whilst the third guarantees that any availability comparison is conservative (i.e. the E-GBAS architecture is expected to perform better than a comparison with the DFree/Konno et al (2006a) method would suggest). Comparing for example, the VAL = 9.5 m requirement to achieve a 99.9% availability for New York (Konno et al., 2006a), an adjustment could be made to the known bias as a result of incorporating E-GBAS to reduce the VAL by  $\sim 4.2$  m. The improvement is due to the fact that in the monitoring proposed in Konno et al (2006a), there is a potential residual bias of 4.2 m as a result of potential undetected ionosphere conditions. Using E-GBAS, it is expected that all conditions would be detected, thereby eliminating this bias. This results in a VAL of  $\sim 5.3$  m for a 99.9% availability (for GPS dual frequency configurations). Furthermore, considering the fact that Galileo dual frequency configurations are expected to have improved error budgets by at least a factor of two with respect to GPS (Schlueter et al, 2005), this would result in an estimated availability of 99.9% for VAL  $\sim 2.65$  m when the E-GBAS configuration is used. Also, it should be noted that the performance evaluation in Konno et al (2006a, 2006b) assumes GPS L1 and L2 and does not account for expected improvements as a result of using modernised GPS L1 and L5 or the Galileo signals. Furthermore, further improvement in availability should be possible if E-GBAS is used in the dual mode as both ionosphere and overall

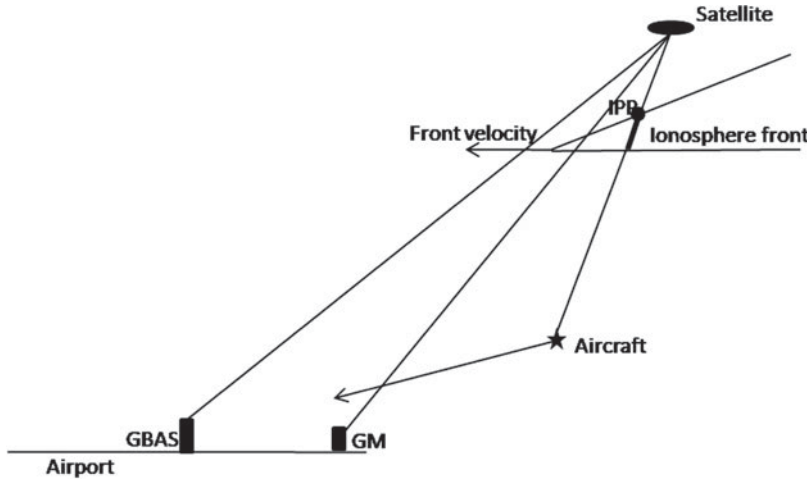


Figure 8. Ionosphere front high-level scheme.

range monitor. Better still, improvement in availability should accrue from the additional reduction in the random part of the ionosphere contribution as a result of using ground-based receivers of the E-GBAS only instead of a combination of ground-based and airborne receivers. E-GBAS also has the potential to act as a detector of irregularities, such as ionospheric scintillation to notify aircraft on the approach of potential failures in the vicinity of the airport. Therefore  $VAL = 2.65$  m for 99.9% availability is expected to be a conservative estimate for this case. While this would potentially enable CAT III performance requirements ( $VAL = 2.6$  m, as proposed by EUROCAE) to be met, it is clear that further research to confirm these findings, and determine if horizontal alert limit requirements ( $HAL = 1.4$  m) for surface movement can also be met with the proposed architecture, is required.

#### 4. E-GBAS CONCEPT VERIFICATION.

4.1. *Simulations.* In order to verify the E-GBAS concept and optimise the layout for specific airports, the following process is proposed: dual-frequency pseudo-range and carrier-phase GPS or/and Galileo signals are simulated with a hardware simulator and recorded at the aircraft for a typical CAT-III approach scenario (including roll-out) as well as taxiing on the ground, at the four reference receiver locations (proposed for the core GBAS CAT III architecture) as well as the GMs strategically placed around the airport. Ionosphere fronts are simulated as follows:

- A delay proportional to the “effective thickness” of the ionosphere front is added to each of the pseudorange measurements.
- The same delay is subtracted from the carrier-phase measurements.

The effective thickness is computed at the ionosphere-pierce-point (IPP) and is taken to be proportional to the transit length of the signal through the ionosphere (shown as a solid thick line in Figure 8), taking into consideration satellite elevation and azimuth as well as the actual geometrical layout of the ionosphere front. This layout

will be defined by a velocity vector describing the direction in which the front is moving and the gradient along this direction. The front-induced errors are simulated with constant TEC values in a direction horizontally perpendicular to the front velocity vector.

The ionosphere induced difference in delay between the user and the GBAS is computed at the GM as a function of time. When the aircraft reaches the threshold, it is co-located with a baseline defined by two GMs. The following tests should be carried out:

- Cross-validation of the computed ionosphere-induced errors at the aircraft-level and the errors computed at the baseline defined by the two GMs providing a baseline closest to the DH, using Equation 2.
- Computation of the aircraft position as a function of time using the differential corrections sent by the core GBAS which have been adjusted for the difference in ionosphere-induced delays between the core GBAS and the GMs.
- Characterisation of the positioning performance as a function of distance from the GMs by comparing the known (simulated) aircraft position with the computed position.

For the CAT-III approach, availability should be computed at the decision height, the point at which the navigation system performance requirements are most stringent, by computing the percentage of time over which the position accuracy and integrity are better than CAT III performance requirements (EUROCAE, 2007) using the approach described in Section 3.1.1. For the taxiing, availability should be computed in the gate-area, where requirements are most stringent and conditions for positioning are worst.

The above procedure should be carried out for varying ionosphere conditions within the maximum threat-space currently observed. In this respect, the gradient should be varied to induce a delay between 0 and 500 mm per km distance between the GBAS core station and the aircraft and the velocity of the front should be varied between 0 and 0.75 km/s.

The following three high-level front scenarios should be considered:

- the velocity vector of the aircraft and the front are aligned and in the same direction;
- the velocity vector of the aircraft and the front are parallel but in opposite directions
- the velocity vector of the front is perpendicular to the aircraft velocity vector.

For the scenarios where the vectors are in the same direction, three principal scenarios should be distinguished: the front is travelling slower, at the same speed and faster than the aircraft. These experiments should be carried out for varying geometrical layouts of the E-GBAS architecture on the airport to optimally trade-off architecture and performance. The whole procedure should be carried out for a GPS-only constellation, a Galileo-only constellation and combined constellations. Furthermore, two separate dual-frequency combinations should be compared: L1/L2 and L1/L5(E5B).

4.2. *On-Site Measurements.* Following the simulation performance characterisation, real on-site experiments should be carried out with the validated E-GBAS optimal architecture. Dual-frequency (either L1/L2 or L1/L5) GPS code and carrier-phase measurements (or/and corresponding Galileo measurements when available)



should be taken at the receiver of an aircraft on a CAT III approach as well as when it is taxiing in the gate-area. Measurements will also be taken at the core GBAS as well as the various GMs. The aircraft receiver will use the adjusted differential GBAS corrections to compute its position. An independent measurement reference, such as suitably placed laser-trackers, is required against which the computed aircraft position can be measured. It is best for these experiments to be carried out during the imminent solar maximum as a validation of the performance under these worst-case conditions. This would provide a pragmatic validation of the E-GBAS concept for more benign conditions.

5. CONCLUSIONS. Current state-of-the-art monitoring architectures are code-based and have shown a number of limitations. Konno et al (2006a, 2006b) developed advanced state-of-the-art rate-based and delay-based monitoring methods and combined these with divergence-free (DFree) smoothing techniques. The CAT III service availability was shown to vary between 96.515% and 99.987% for a VAL = 10 m for select locations across the CONUS. Smaller VAL necessarily result in performance degradation and, as a result, this method is not expected to be able to meet the significantly more stringent EUROCAE CAT III requirements. Whilst a dual-frequency Galileo configuration would provide improved results, it is not expected that the proposed method would be able to meet the CAT III requirements, essentially because it needs to make assumptions about worst case ionosphere biases which significantly limit its performance. The IFree method developed in Konno et al. (2006b) has limited availability as a result of the large noise of the observables used. Results in Konno et al. (2006b) suggest that with a GPS dual-frequency configuration, EUROCAE CAT III requirements cannot be met. Further studies are required to determine if the improved code modulation (and significantly improved error budgets) of Galileo would enable the IFree method to provide the necessary availability with a Galileo-only or a GPS + Galileo dual-frequency configuration. In this regard, of particular interest would be a study investigating the required SIS performance of Galileo in order to reach the EUROCAE CAT III requirements with the IFree method.

The uncertainty surrounding current methods triggered the development of a reliable alternative, using a carrier-phase and ground-only based E-GBAS monitoring architecture. DFree + E-GBAS has been shown to have the potential to provide a significant improvement over current proposed architectures. This improvement should satisfy EUROCAE CAT III landing navigation and potentially taxiing requirements. However, a potential drawback of this architecture is its increased complexity. Further studies are required to verify these findings.

## REFERENCES

- Datta-Barua, S. et al. (2006). *Bounding Higher Order Ionosphere Errors for the Dual Frequency GPS User*, ION GNSS.
- EUROCAE, (2007). *High-Level Performance Requirements for a Global Navigation Satellite System/Ground Based Augmentation System to Support Precision Approach Operations*, ED-144, EUROCAE WG28 SG4.
- Hofmann-Wellenhof et al., (2001). *GPS – Theory and Practice (5<sup>th</sup> ed.)*, Springer-Verlag.



- Konno, H. et al., (2006a). *Ionosphere Monitoring Methodology for Hybrid Dual-Frequency LAAS*, ION GNSS, Fort-Worth.
- Konno, H. et al., (2006b). *Evaluation of Two Types of Dual-Frequency Differential GPS Techniques under Anomalous Ionosphere Conditions*, ION NTM, Monterey.
- Liu, X., Tiberius, C., De Jong, K., (2004). *Modelling of differential single difference receiver clock bias for precise positioning*, GPS Solutions.
- RTCA, *Minimum Aviation System Performance Standards for the Local Area Augmentation System (LAAS)*, RTCA-DO245A
- Schlueter, S., Bauer, T., Schuster, W., (2005). *Critical Analysis of Space Based Navigation Technologies Usable for Civil Aviation*, ANASTASIA Deliverable D3.1
- Skone, S. et al., (2005). *Investigating the Impact of Ionospheric Scintillation Using a GPS Software Receivers*, ION GNSS